Supporting Information to

"Heterogeneities of the Nanostructure of Pt/Zeolite Y Catalysts Revealed by Electron Tomography"

*Jovana Zečević,[†] Ad M. J. van der Eerden, [†] Heiner Friedrich,[‡] Petra E. de Jongh,[†] and Krijn P. de Jong[†,]**

[†] Inorganic Chemistry and Catalysis, Debye Institute for Nanomaterials Science, Utrecht University, Universiteitsweg 99, 3584 CG Utrecht, The Netherlands, and [‡] Laboratory of Materials and Interface Chemistry, Department of Chemical Engineering and Chemistry, Eindhoven University of Technology, Den Dolech 2, 5612 AZ Eindhoven, The Netherlands

*Address correspondence to k.p.dejong@uu.nl

1. Experimental

N_2 physisorption. N_2 adsorption and desorption measurement of the samples outgassed in nitrogen flow at 300 °C for 14 h were performed on a Micromeritics TriStar 3000 at liquid nitrogen temperature. To obtain micropore and mesopore volumes, the t-plot and the Barrett–Joyner–Halenda (BJH) methods were used, respectively.

TEM and Electron Tomography. TEM imaging was performed on a Tecnai 12 (FEI, 120kV) transmission electron microscope. Electron tomography experiments were performed on a Tecnai 20 (FEI) transmission electron microscope operated at 200 kV in bright field imaging mode. Sample preparation consisted of crushing and suspending the powder in ethanol by sonication. A few droplets of the suspension were applied on a Quantifoil R2/1 Cu TEM support grid which already contained 5 nm Au particles on top of a thin carbon film. Series of images of different crystals were recorded with a bottom-mounted TVIPS CCD camera over an angular range of about ± 75° at tilt increments of 2°. Depending on the size of the crystal, imaging was done at nominal magnifications of 50,000, 62,000 or 80,000 times. Acquired tilt images were aligned to a common origin and rotation axis by tracking the Au particles, binned by a factor 2 to facilitate further computation and submitted to 3D-reconstruction using a WBP (Weighted Back Projection) algorithm in IMOD[1]. In accordance with the magnification experiments were carried out at, final reconstructions had a voxel size of $(0.20\ nm)^3$, $(0.26\ nm)^3$ or $(0.32\ nm)^3$.

Image analysis. Image processing was performed in Matlab using the DipLib toolbox (www.diplib.org). 3D-reconstructed volumes were first processed with a median filter in order to

reduce noise. In case of preparing the reconstructed volumes for Pt particle segmentation, the size of the median filter element was set to 3-5 in order to preserve details for the small Pt particles. A larger median filter size of 10 was used when preparing the volumes for the zeolite crystal segmentation. As a next step, different threshold values were applied to filtered reconstruction volumes to segment (isolate) Pt particles and zeolite crystal, and hence obtain their binarized volumes. The binarized zeolite volumes were submitted to further morphological operations (*e.g.* dilation, erosion) in order to reduce artifacts originating from the noise, while the Pt binarized volumes were used without further processing. Pt particles of less than 3 voxels in diameter were excluded from the analysis on account of sampling limitations; while for all other Pt particles their volume and coordinates were determined for further quantitative analysis. Due to the limited angular range (*ca.* ± 75°), at which crystals were imaged, the resolution along the z-axis is impaired by elongation of the reconstruction point-spread function. To reduce the impact of elongation on the quantitative results, volumes of Pt particles were divided by an elongation factor e_{yz} prior to further calculation.[2] Pt size distributions were obtained after calculating diameters of individual Pt particles from elongation corrected Pt volumes by assuming a spherical shape. Surface-to-surface distances between nearest neighbor Pt particles were obtained by, first, determining the shortest center-to-center distances based on center of mass coordinates of each Pt particle, followed by subtraction of corresponding radii of the Pt particles to which the shortest distance applies. Pt loadings (in wt %) of individual zeolite crystals were calculated based on volumes derived from Pt and zeolite segmentations and the bulk densities of metallic Pt and zeolite Y with Si/Al=30. Volume and isosurface rendering resulting in interactive color representations of segmented volumes were performed using Amira software.

EXAFS. The extended X-ray absorption fine structure (EXAFS) Pt L_3 edge measurements were performed at Beamline C of the HASYLAB synchrotron (Hamburg, Germany). All measurements, as described previously,[3] were performed in transmission mode, with incident and transmitted X-ray beams detected by ionization chambers filled with a N_2/Ar gas mixture. The gas mixtures were adjusted to absorb 20 % of the intensity of the incident beam and 80 % of the intensity of the transmitted beam. To reduce the higher harmonics contribution, the Si(111) double crystal monochromator was detuned to 50 % maximum intensity. Calibration of the beam energy was performed by using a platinum foil between the second and third ionization chamber. The appropriate amount of sample was measured in order to achieve total absorbance of 2.5, pressed into a self-supporting wafer and placed in a cell operated at atmospheric pressure. Prior to the measurements, the pre-reduced sample which had been carefully passivated, was re-reduced in a flow of pure H_2, during heating with 5 ^{o}C/min to 200 ^{o}C and 20 min at that temperature (sufficiently high for reduction of Pt). Afterwards, the cell was cooled to room temperature, disconnected from the gas flow with overpressure and cooled down to liquid nitrogen temperature at which the EXAFS measurements were performed. The background subtraction of the adsorption data was performed using standard procedures. The pre-edge background was approximated by a modified Victoreen curve, the post-edge background was subtracted using cubic spline routines and normalization was performed by dividing the data by the magnitude of the edge jump determined at 50 eV above the edge energy. Data was analyzed by multiple shell fitting in *R*-space ($1.5 < R < 3.2$ Å, $2.5 < k < 17$ Å^{-1}, *k*-weighting 1) using the data analysis package XDAP. The variances in imaginary and absolute parts, as well as a control calculation with *k*-weight 3 were used to determine the fit quality. The individual backscatterers were identified by applying the difference-file technique using phase- and amplitude corrected

Fourier transforms. The references compounds for the phase shifts and backscattering amplitudes were theoretical Pt-Pt and Pt-O references generated by the FEFF7 code and calibrated with experimental spectra of Pt-foil and $Na_2Pt(OH)_6$.

Inductively Coupled Plasma (ICP) analysis. Pt elemental analysis has been performed at Kolbe Mikroanalytisches Laboratorium (Mülheim and der Ruhr, Germany) using an ICP-OES Perkin Elmer spectrometer after sample dissolution according to standard in-house procedures.

2. Textural properties of HY30 and Pt-HY30 samples

N_2 adsorption and desorption measurements of pristine HY30 support and Pt-HY30 sample were performed under conditions described in the Section 1 of the Supporting Information.

Hysteresis loop of the adsorption and desorption isotherms (Figure 2.1a) points to presence of mesopores, while the closure of this loop at about 0.45 relative pressure indicates that some of the present mesopores are blocked. Blocked mesopores are either cavity-like and can be accessed only through micropore network, or they are constricted and accessible through openings of 3-4 nm. It was shown, however, that this type of support possesses mainly open type of mesopores.[4]

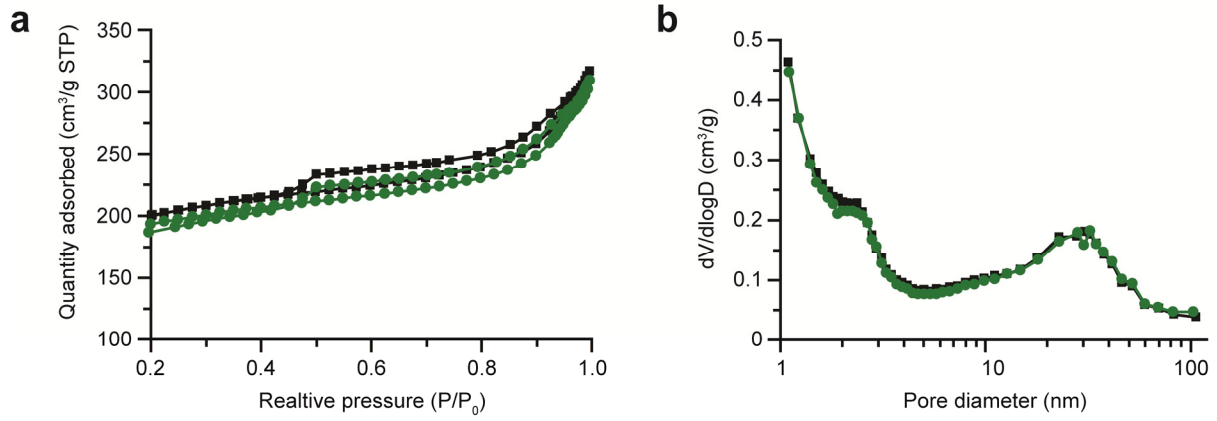

Figure 2.1. N_2 physisorption analysis of HY30 (black) and Pt-HY30 (green) samples. (a) Adsorption and desorption isotherms. (b) BJH pore size distribution derived from the adsorption branch.

Barrett–Joyner–Halenda (BJH) pore size distribution derived from the adsorption branch (Figure 2.1b) shows that majority of mesopores have broad size distribution around 20-30 nm diameter, while the small peak just over 2 nm implies that some small mesopores are present as well.

Table 2.1 summarizes the obtained textural properties. As can be seen the introduction of Pt particles causes no change in the textural properties of the support. Negligible variations in values are within measurement error.

Table 2.1. Textural properties of HY30 support and Pt loaded HY30.

	S_{meso}[a] [m^2/g]	V_{micro}[b] [cm^3/g]	V_{meso}[c] [cm^3/g]	V_{tot}[d] [cm^3/g]
HY30	225	0.21	0.18	0.49
Pt-HY30	212	0.21	0.18	0.48

[a] Surface area. [b] Micropore volume. [c] Mesopore volume. [d] Total pore volume.

3. Non-mesoporous zeolite HY supported Pt

In order to determine whether it is possible for Pt particles to locally destroy the structure of the zeolite crystal upon growth, an additional set of experiments was performed. Here non-mesoporous zeolite Y in H-form was used as a support. HY zeolite was obtained by calcining the NH_4-form of zeolite Y with the Si/Al ratio of 2.6 (Zeolyst, CBV300) following commonly used conditions.[5–7]

To confirm the absence of mesopores N_2 physisorption was performed on both NH_4Y and HY powders. As can be seen in Figure 3.1 there is a flat curve and no hysteresis, indicating that mesopores are absent from both pristine NH_4Y zeolite powder and HY zeolite derived thereof.

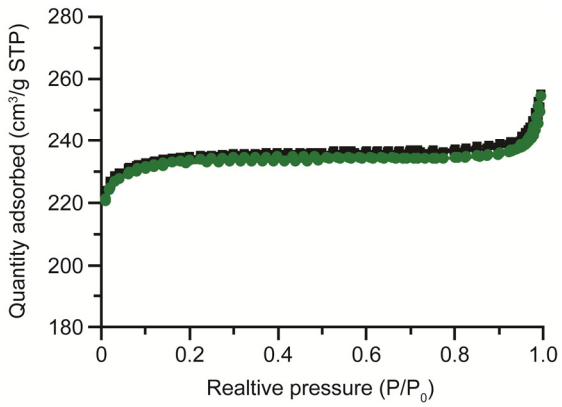

Figure 3.1. N_2 adsorption and desorption isotherms of NH_4Y (black) and HY (green) powders.

Pt-HY samples were prepared following the conditions described in the manuscript for the preparation of Pt-HY30 and Pt-HY30-R samples. That is, obtained HY powder was impregnated with $Pt(NH_3)_4(NO_3)_2$ aqueous solution to nominal 1 wt% Pt loading. The incipient wetness impregnation method was used, after which the powder was dried and subjected to two different heat treatments. One involved calcination in air flow (~5000 GHSV) at 350 °C for 2 h followed

by reduction in H_2 flow at 600 °C for 3 h, which resulted in Pt-HY sample. The second involved direct reduction in H_2 flow at 600 °C for 3 h to promote Pt particles growth (Pt-HY-R sample).

Figure 3.2 shows slices from the middle of the reconstructed volumes of Pt-HY and Pt-HY-R samples. It is apparent that in case of Pt-HY sample small (~1 nm) Pt particles are formed and are uniformly distributed throughout the zeolite crystal (Figure 3.2a). When direct reduction was applied in case of Pt-HY-R sample, the size of Pt particles increased to 3-4 nm as expected (Figure 3.2b). These larger Pt particles are also uniformly distributed inside the zeolite crystal and appear to be entrapped in the microporous regions. Please note that the white streaks appearing on the sides of Pt particles are common artifacts of the weighted back-projection reconstruction and are not indicative of actual mesopores.

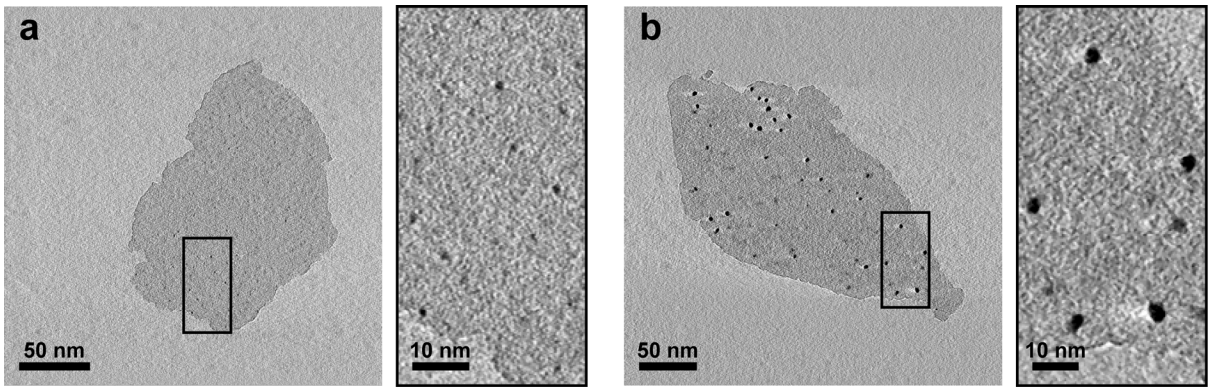

Figure 3.2. Slices through the reconstructed volumes of (a) Pt-HY sample, recorded at 62,000 times magnification and (b) Pt-HY-R sample, recorded at 50,000 times magnification.

As there are no small mesopore cavities in this material, it can be argued that upon growth Pt particles cause local destruction of zeolite structure. This means that for accommodating 3-4 nm Pt particles, the wall between two neighboring micropores should collapse leaving a cavity of similar size. Earlier study also implied a tendency of zeolite Y to undergo creation of defects of this size range.[8]

4. The influence of pelletizing powder

To investigate whether changing the sample preparation conditions can have an influence on the Pt size distribution and zeolite loading, additional samples were prepared. Impregnated zeolite powder was pressed into a pellet, crushed and sieved to 70-40 mesh fractions and submitted to calcination in air flow at 350 °C for 2 h with a 0.5 °C/min ramp. Reduction was done in H_2/N_2 1:1 gas mixture flow at 600 °C for 3 h with a 5 °C/min ramp. Detailed ET and image analysis study of this Pt-HY30(pel) sample ('pel' denotes fractioned pellet form) showed qualitative and quantitative results (Supporting Figure S2) similar to the powdered version of the sample discussed in the main body of the manuscript. A narrower Pt size distribution with somewhat lower mean Pt diameters was observed compared to the powdered version of the sample (Supporting Figure S4a, where summarized Pt histograms for all examined crystals are presented). Variation in Pt loading between crystals was again pronounced, ranging from 0.5 wt% to 7.2 wt%, while Inductively Coupled Plasma (ICP) analysis of the bulk sample confirmed the Pt loading of 1.3 wt%.

Another batch of pelletized impregnated zeolite was submitted to direct reduction under H_2/N_2 1:1 gas flow at 600 °C for 3 h with the ramp of 5 °C/min to obtain Pt-HY30-R(pel) sample. Results from ET and image analysis (Supporting Figure S3) showed that the volume averaged Pt diameters are lower (1.8 - 2.1 nm) when compared to Pt-HY30-R sample described in the manuscript (2.7-4.5 nm). Narrower, *i.e.* more homogeneous, Pt size distributions were observed among Pt-HY30-R(pel) crystals compared to the more broad and inhomogeneous Pt size distributions within crystals of corresponding powdered sample (Supporting Figure S4b). This detailed 3D analysis of the zeolite crystals highlights the potential impact of macroscopic

phenomena, such as hydrodynamics of the gas (air of H_2 during heat treatments) flow through powdered or pelletized samples, on local nanoscale properties (*e.g.* Pt size distribution) that can further have a huge impact on overall catalytic performance. A large variation in Pt loading was again observed (0.4-3.5 wt%) even though ICP analysis pointed to 1.2 wt% Pt loading of the bulk sample.

In order to compare the electron tomography results obtained at the nanoscale with bulk properties, extended X-ray absorption fine structure (EXAFS) measurements were performed on both pelletized samples (see Figure 4.1 below).

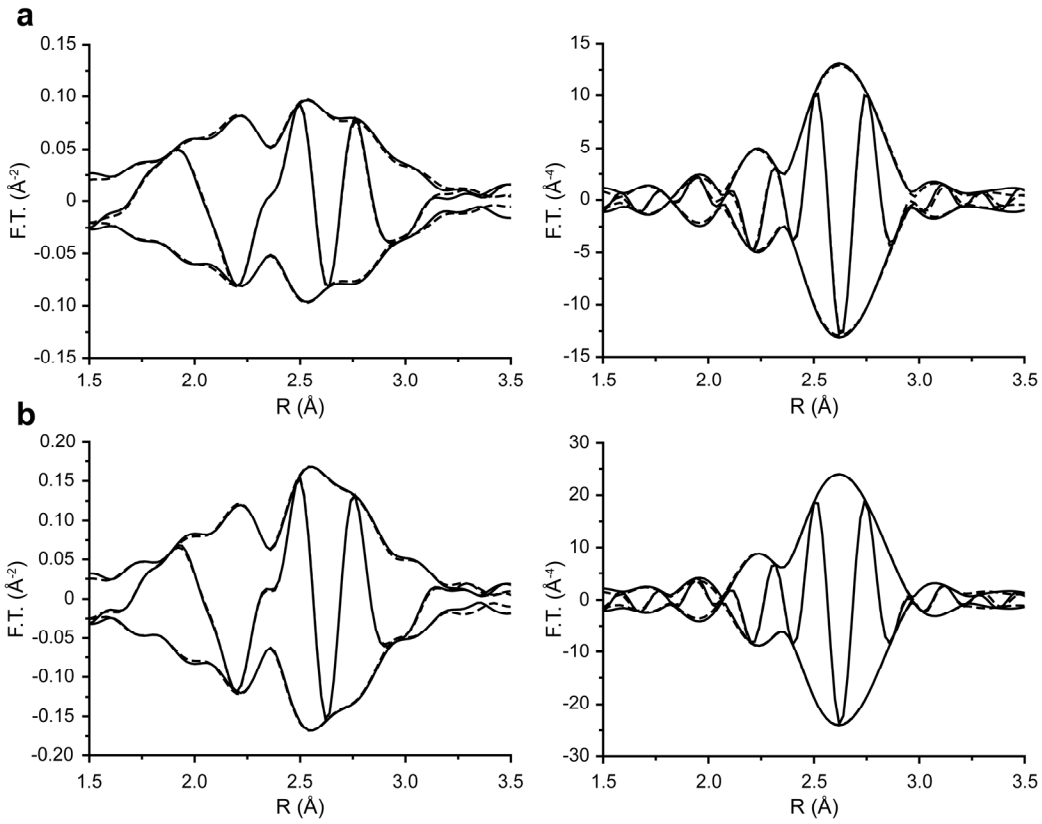

Figure 4.1. Fourier transforms k^1-weighted (left side) and k^3-weighted (right side), Δk 3.5-17 $Å^{-1}$, of the raw data (solid line) and the total fit, fit area 1.5-3.2 Å (dotted line), of the samples Pt-HY30(pel) (a) and Pt-HY30-R(pel) (b).

The EXAFS results, summarized in the below presented Table 4.1, show that Pt coordination number in Pt-HY30(pel) sample is only 5.68, which translates into very small ~ 0.9 nm Pt particles if a spherical shape of the particles is assumed. A larger average Pt diameter of 2.0 nm was calculated for the Pt-HY30-R(pel). These values are in good agreement with the volume averaged Pt diameters calculated from the ET studies, ranging from 0.9 to1.2 nm for the Pt-HY30(pel) and from 1.8 to 2.1 nm for the Pt-HY30-R(pel) samples.

Table 4.1. Fit parameters and results of EXAFS spectra.

Sample	Shell	Scatterer	N	$\Delta\sigma^2$ (10^{-3} Å^2)	R (Å)	ΔE_o (eV)
Pt-HY30(pel)	1	Pt	5.68	2.2	2.76	0.94
	2	O	0.68	8.4	2.17	-14.75
Pt-HY30-R(pel)	1	Pt	8.31	1.4	2.76	0.91
	2	O	0.43	2.0	2.14	-14.11

Supporting Information References

1. Kremer, J. R.; Mastronarde, D. N.; McIntosh, J. R. Computer Visualization of Three-Dimensional Image Data Using IMOD. *J. Struct. Bio.* **1996**, *116*, 71–76.

2. Friedrich, H.; Sietsma, J. R. A.; Jongh, P. E. de; Verkleij, A. J.; Jong, K. P. de Measuring Location, Size, Distribution, and Loading of NiO Crystallites in Individual SBA-15 Pores by Electron Tomography. *J. Am. Chem. Soc.* **2007**, *129*, 10249–10254.

3. Zečević, J.; Eerden, A. M. J. van der; Friedrich, H.; Jongh, P. E. de; Jong, K. P. de H2PtCl6-Derived Pt Nanoparticles on USY Zeolite: A Qualitative and Quantitative Electron Tomography Study. *Microporous Mesoporous Mater.* **2012**, *164*, 99–103.

4. Zečević, J.; Gommes, C. J.; Friedrich, H.; Jongh, P. E. de; Jong, K. P. de Mesoporosity of Zeolite Y: Quantitative Three-Dimensional Study by Image Analysis of Electron Tomograms. *Angew. Chem., Int. Ed.* **2012**, *51*, 4213–4217.

5. Li, D. Zeolite-Supported Ni and Mo Catalysts for Hydrotreatments II. HRTEM Observations. *J. Catal.* **2000**, *189*, 281–296.

6. Sato, K.; Nishimura, Y.; Honna, K.; Matsubayashi, N.; Shimada, H. Role of HY Zeolite Mesopores in Hydrocracking of Heavy Oils. *J. Catal.* **2001**, *200*, 288–297.

7. Kuznetsov, P. Study of N-octane Hydrocracking and Hydroisomerization over Pt/HY Zeolites Using the Reactors of Different Configurations. *J. Catal.* **2003**, *218*, 12–23.

8. Jong, K. P. de; Zečević, J.; Friedrich, H.; Jongh, P. E. de; Bulut, M.; Donk, S. van; Kenmogne, R.; Finiels, A.; Hulea, V.; Fajula, F. Zeolite Y Crystals With Trimodal Porosity as Ideal Hydrocracking Catalysts. *Angew. Chem., Int. Ed.* **2010**, *49*, 10074–10078.

5. Supporting Figures S1-S4

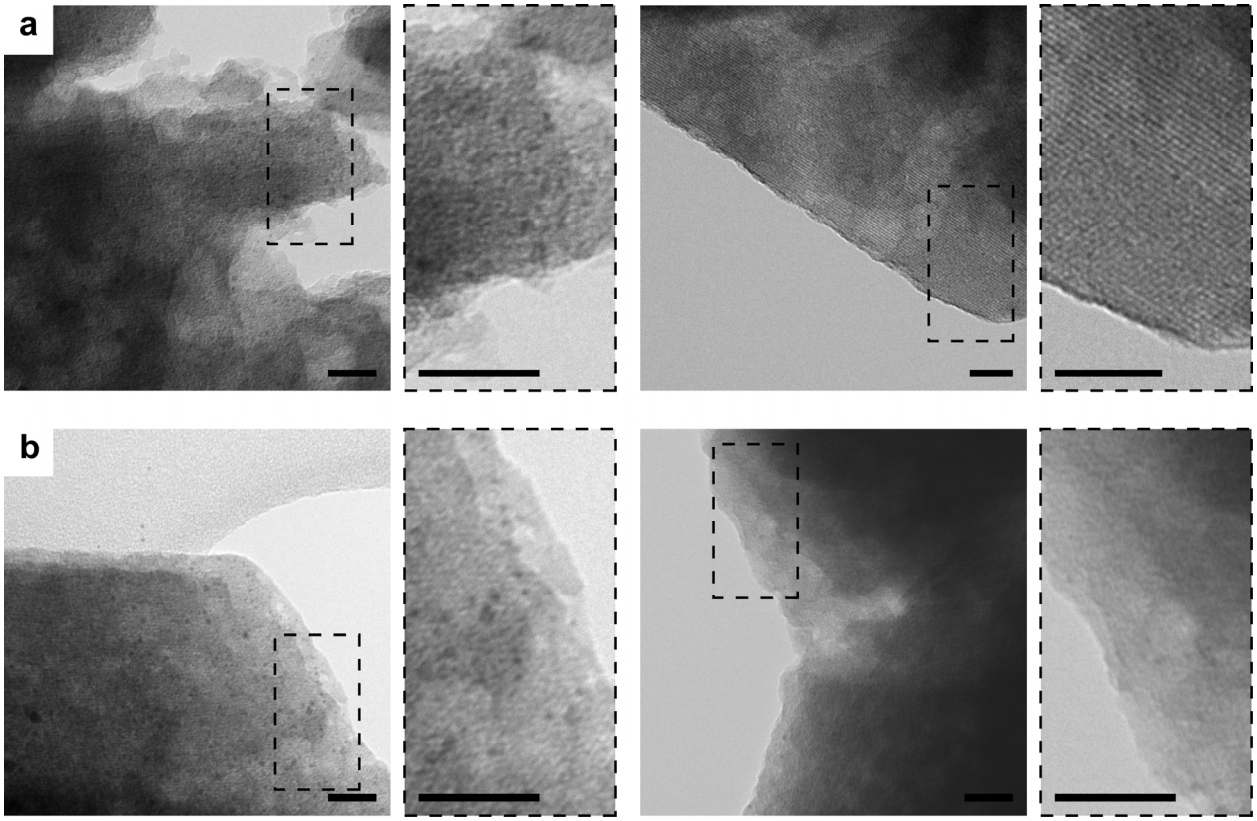

Supporting Figure S1. TEM micrographs of Pt-HY30 samples showing loaded zeolite crystals with small ~1 nm Pt particles inside zeolite crystals (left) and zeolite crystals that appear to be less loaded with Pt (right). (a) Sample prepared with calcination in air flow and subsequent reduction in H_2 at 600 °C. (b) Sample prepared in air flow and subsequent reduction in H_2 at 650 °C. Scale bars are 20 nm.

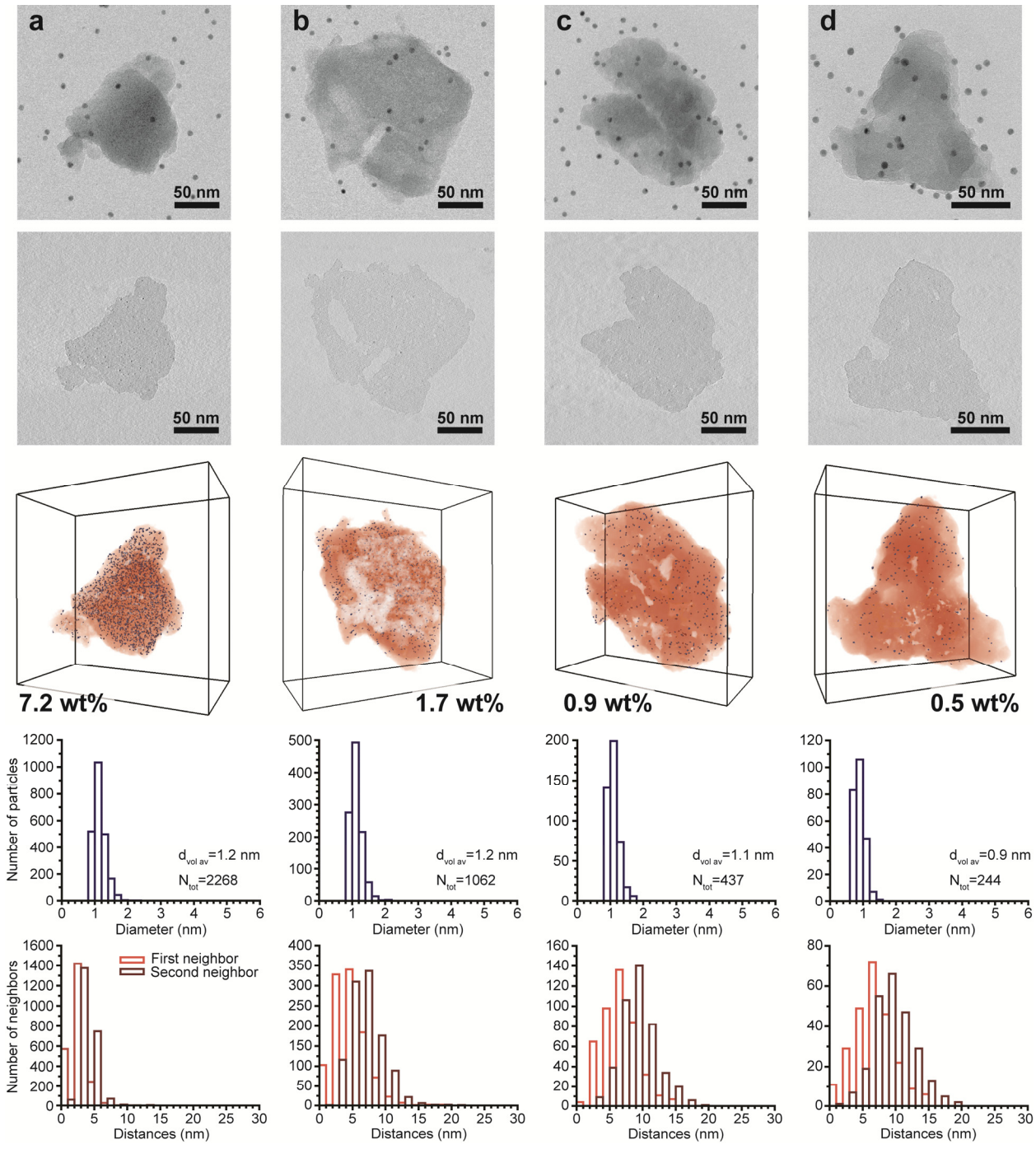

Supporting Figure S2. Electron tomography and image analysis of various Pt-HY30(pel) crystals recorded at 62,000 (a-c) and 80,000 times (d) magnification. In the first row TEM micrographs taken at 0° tilt angle are shown. The second row presents 0.26 nm (a-c) and 0.20 nm (d) thick slices from the reconstructed volumes of crystals from the first row. In the third row volume and isosurface rendered representations of crystals with calculated Pt loadings are shown, where zeolite crystals are in orange, Pt particles in blue and mesopores in white. Pt size distribution and surface-to-surface distances of the first and the second nearest neighboring Pt particles are presented in rows 4 and 5.

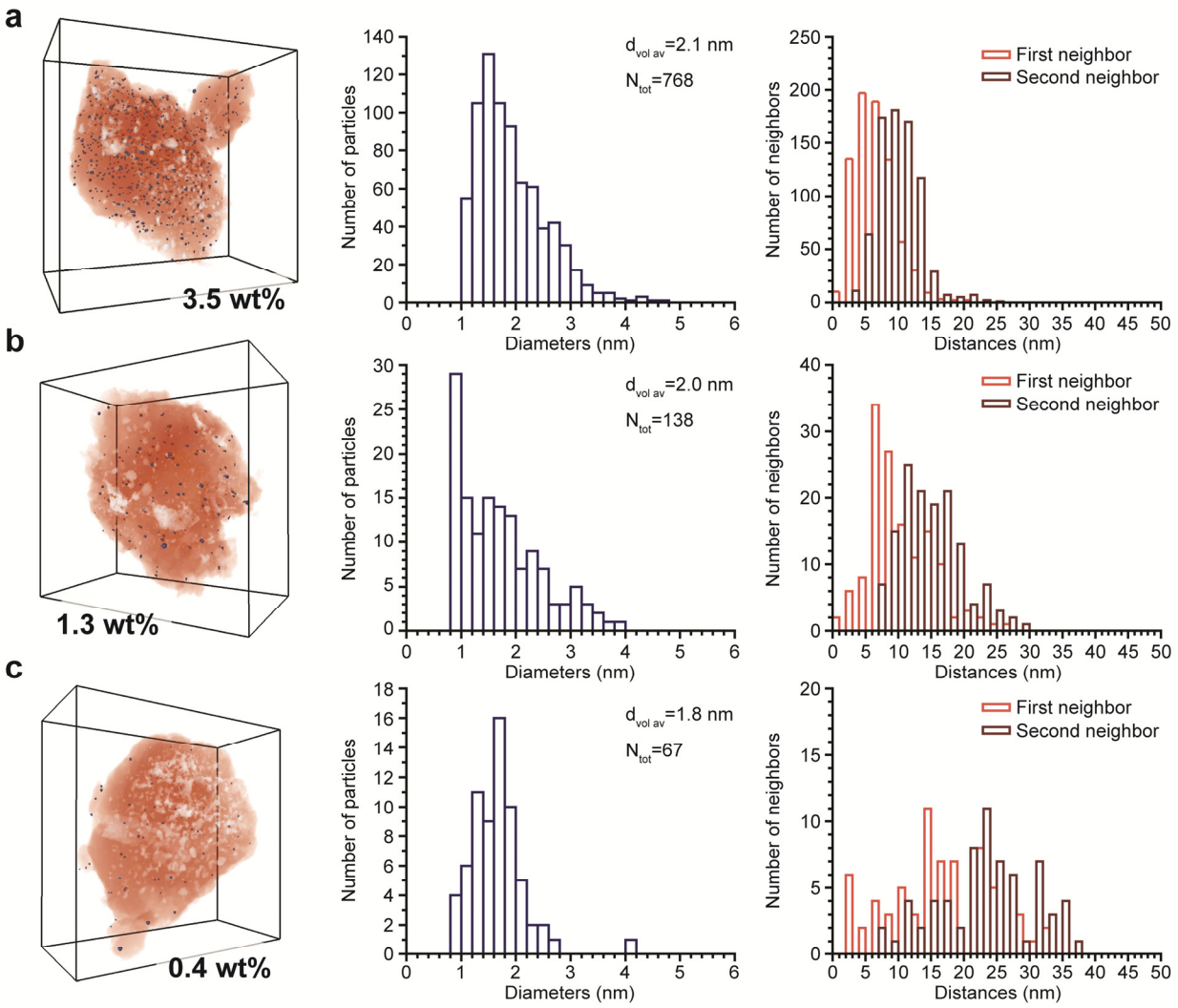

Supporting Figure S3. Image analysis of a few (a-c) reconstructed Pt-HY30-R(pel) crystals. Volume and isosurface rendering showing segmented Pt particles (blue), zeolite crystal (orange) and mesopores (white) are shown at the right hand side with denoted calculated Pt loadings of each crystal. In the center, Pt size distributions of crystals (a-c) are presented, while on the right hand side surface-to-surface distances of the first and the second nearest neighboring Pt particles are shown.

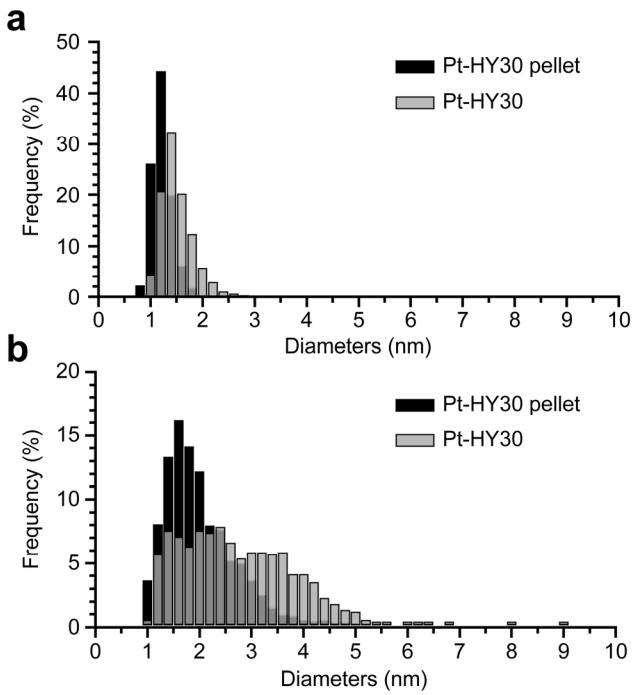

Supporting Figure S4. Comparison of Pt size distributions derived from image analysis of all imaged Pt-zeolite crystals of samples submitted to heat treatments in either powder form or fractioned pellet form. (a) Calcination and reduction of Pt impregnated pelletized Pt-HY30 sample (black) leads to narrower Pt size distribution when compared to powdered sample (grey) that underwent the same heat treatments. (b) Direct reduction of Pt impregnated pelletized sample Pt-HY30-R (black) leads to narrower Pt size distribution with smaller mean Pt diameter when compared to directly reduced powdered sample (grey). The positive influence of direct reduction on Pt nanoparticles growth in both powdered and pelletized samples is apparent when histograms from (a) and (b) are compared.

6. Supporting Movies 1-2

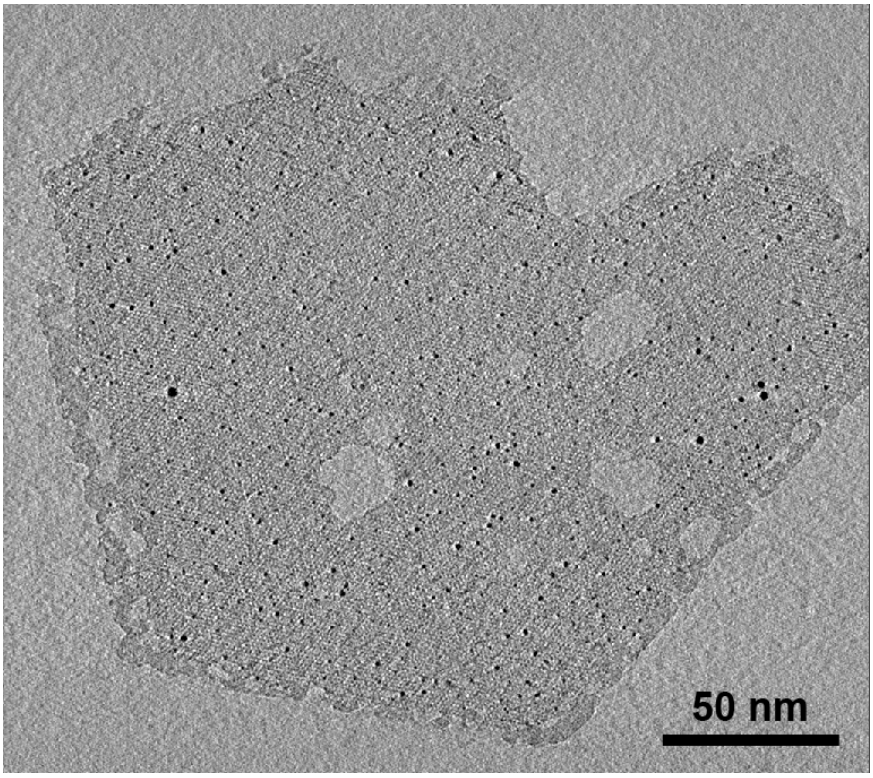

Supporting Movie 1. Showing set of 0.32 nm thick slices along the height of the reconstructed volume of Pt-HY30 crystal. Pt particles of ~1 nm (small black dots) seem to be well distributed throughout the microporous crystalline region of zeolite (darker grey), while mesopores (light grey) are empty. Due to restrictions in file size, movie was compressed which degraded the resolution.

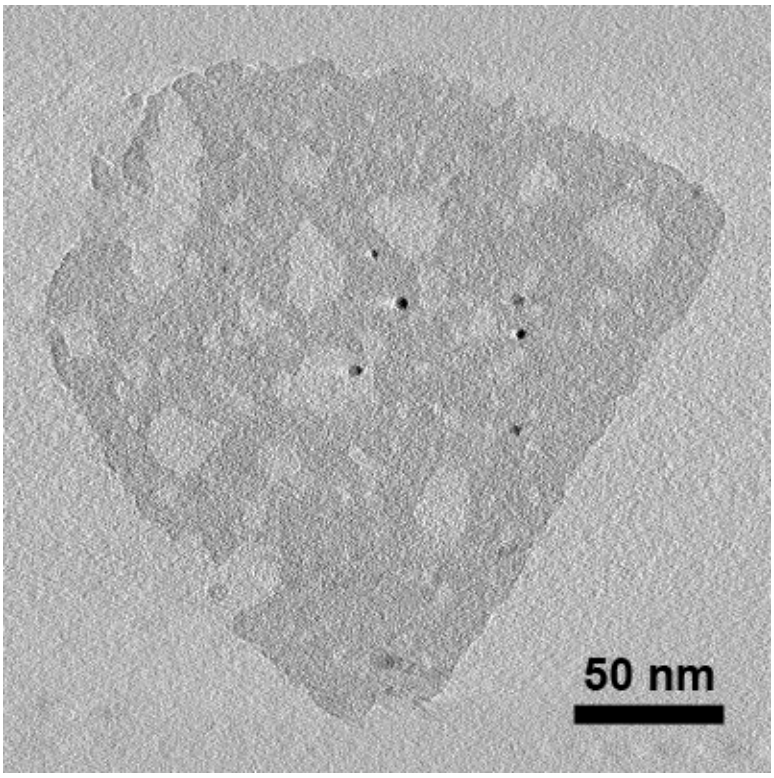

Supporting Movie 2. Showing set of 0.32 nm thick slices along the height of the reconstructed volume of Pt-HY30-R crystal. Even though Pt particles are ~ 3 nm (black dots) which is larger than the size of zeolite Y micropore cavities (1.2 nm), they are mainly located inside microporous crystalline region of zeolite (darker grey), while mesopores (light grey) remain empty. White streaks appearing on the sides of Pt particles are artifact of the weighted-back-projection technique and should not be mistaken for mesopores. Due to restrictions in file size, movie was compressed which degraded the resolution.